Volume 12 Number 15 1984 Nucleic Acids Research

Viroid replication: equilibrium association constant and comparative activity measurements for the viroid-polymerase interaction

Thomas C.Goodman*, Luitgard Nagel, Winfried Rappold**, Günther Klotz+ and Detlev Riesner#

Institut für Physikalische Biologie, Universität Düsseldorf, D-4000 Düsseldorf, and +Abteilung für Virologie, Universität Ulm, D-7900 Ulm, FRG

Received 12 June 1984; Accepted 16 July 1984

ABSTRACT

The binding and replication of purified potato spindle tuber viroid (PSTV) by DNA-dependent RNA polymerase II from wheat germ was studied in analytical ultracentrifugation experiments and in vitro transcription assays. The equilibrium association constant for the viroid-polymerase interaction is 1.9×10^7 M^{-1}. Both ultraviolet and fluorescent monitoring during the sedimentation experiments showed two distinguishable viroid-polymerase complexes. These are interpreted as resulting from a 1:1 and 2:1 enzyme-to-viroid binding stoichiometry. A_{265}/A_{280} ratios across the sedimenting boundaries, the sedimentation velocity of the complexes, as well as electron microscopic data support this interpretation. The role of viroid secondary structure in enzyme binding and polymerization is discussed in the light of these results and compared with binding and polymerization data for virusoid RNA, single- and double-stranded RNA, and double-stranded DNA.

INTRODUCTION

Viroids are single-stranded, covalently closed circular RNA molecules. As a class of pathogens, they are distinguished from viruses by their small size (approx. 360 nucleotides) and lack of any capsule or protein coat (reviewed in 1-4). Viroids are observed to infect a variety of higher plants including potato, tomato, and coconut palm and can cause significant agricultural damage. Viroids or "viroid-like" agents have also been implicated in animal and human diseases, however, no definitive evidence for viroid hosts other than higher plants has yet been obtained.

The primary nucleotide sequence and secondary structure has been determined for a number of different viroids (1,6-7). In all cases, viroids are observed to adopt rod-like structures where regions of intramolecular base pairing alternate with loops in an unbranched arrangement (7,8). Viroids do not exhibit tertiary structures and have been characterized both with regard to the thermodynamics and kinetics of their structural transitions and their hydrodynamic behavior in sedimentation experiments (reviewed in 9,10).

While a great deal is known about the structure of viroids, relatively less

is known of the detailed process and enzymology of viroid replication. Viroids are most likely replicated by host specific enzymes. The small size of viroids, their lack of long open reading frames, and the absence of viroid-specific polypeptides all suggest this. In addition, a number of lines of positive evidence point to the specific involvement of the DNA-dependent RNA polymerase II in at least the early stages of viroid replication. The fungal toxin, α-amanitin, is known to inhibit RNA polymerases and has been shown to inhibit viroid replication at in vivo concentrations as low as 10^{-8} M (11). DNA-dependent RNA polymerase II preparations from both wheat germ and tomato plant tissues are also able to produce full length viroid RNAs in vitro (12).

Since rigorous hybridization experiments have ruled out the presence of viroid sequences integrated within the host genome (13,14), it appears that the viroid molecule is directly recognized by the host cell enzyme. Larger than unit length viroid minus strands have been shown to be present in infected plants (15-17), and a rolling circle model for replication has been suggested to accommodate the available data (17-18).

In this paper we employ a model system composed of purified potato spindle tuber viroid (PSTV)[1] and DNA-dependent RNA polymerase II isolated from wheat germ to determine the equilibrium association constant and stoichiometry of the viroid polymerase interaction. We demonstrate that polymerase binding to viroid is stronger than would be expected for a non-specific protein-nucleic acid interaction. We show that the polymerizing activity of the enzyme is largely independent of viroid secondary structure, and we compare the relative affinity of the polymerase for viroid RNA and other RNA and DNA templates. These data suggest that the DNA-dependent RNA polymerase II specifically recognizes and binds a viroid RNA sequence. Transcription of the viroid RNA by this enzyme is likely an important facet of the overall process of viroid replication.

MATERIALS AND METHODS

Nucleic Acids

Potato spindle tuber viroid (PSTV) was prepared by a combination of Cs_2SO_4 density gradient centrifugation and HPLC as described (19,20). Concentrated PSTV stock solutions were typically 10-20 A_{260}/ml in a buffer containing 1 mM Na-cacodylate, pH 7.0, 10 mM NaCl, and 0.1 mM EDTA. All buffers were prepared from high purity water (Milli-Q-System, Millipore GmbH). Prior to use, viroid aliquots were heated to 50°C for 5 min and then allowed to cool to room temperature. This procedure was necessary to resolve transient intra- and

intermolecularly base paired structures. Viroid preparations employed in this study were analyzed by denaturing polyacrylamide gel electrophoresis (21). All samples contained greater than 95% circular molecules. Contamination by other RNA species was less than 1% as judged by the gel electrophoresis in combination with nucleic acid silver staining (21).

Velvet tobacco mottle virus (VTMoV) was generously provided in total RNA extract form by J.W. Randles and R.H. Symons (University of Adelaide, Australia). The circular virusoid RNA2 molecule from VTMoV (22,23) was purified away from other species essentially as described for viroid RNAs (20). Double and single-stranded necrotic cucumber mosaic virus-associated RNA5 (dsCARNA5 or ssCARNA5, respectively) were a gift of J. Kaper (24,25). The 187-bp DNA restriction fragment used in these studies was prepared as described (26). Calf thymus DNA was purchased from Sigma and t-RNA^{phe} from E. coli was from Boehringer Mannheim.

DNA-dependent RNA polymerase II

DNA-dependent RNA polymerase II from wheat germ (E.C. 2.7.7.6) was purified and stored as described (27-29). Raw wheat germ was provided as a gift from the Plange Mills (Düsseldorf, FRG). Ethylene glycol used in the column chromatography was purchased from Merck (Darmstadt, FRG); glycerol (99.5%) was from Roth (Karlsruhe, FRG); Polymin P and $(NH_4)_2SO_4$ (enzyme grade) were obtained from BRL (Gaithersburg, MD, USA). Filtration assays characterizing successive steps in the enzyme purification procedure were as described (27) except that 1 µCi of (α-^{32}P)UTP (Amersham, Braunschweig, FRG) at a specific activity of 10 µCi/nmole was used per assay.

Analytical ultracentrifugation

Analytical ultracentrifugation experiments were performed in a Spinco model E ultracentrifuge equipped with a high intensity ultraviolet illumination system, photoelectric scanner, and electronic multiplexer (30). Depending on the concentrations of the components in the experiment, charcoal-filled epon centerpieces of either 3 or 12 mm were chosen. Unless otherwise indicated, the velocity sedimentation experiments employed a buffer solution containing 25 mM Tris-HCl, pH 7.9, 25% glycerol, 50 mM NaCl, 6 mM $MgCl_2$, 1 mM EDTA, and the indicated concentrations of sedimentating components. Experiments were performed at 20°C and 48,000 rpm. Absorbance ratios, A_{265}/A_{280}, were obtained for sedimentating bands during the actual sedimentation experiment as previously described (31).

A fluorescence detection system for analytical ultracentrifugation experiments has been developed in our laboratory (32). This instrument employs a 4

watt argon laser (Spectra Physics Model 164) in conjunction with a Spinco model E analytical ultracentrifuge to allow the observation of sedimenting species by their fluorescence emissions. In experiments performed with this instrument ethidium bromide or ethidium homodimer (Fluka, Ulm, FRG) was intercalated in the viroid structure. The 514.5 nm laser line was used to excite the fluorochrome. The laser was focused to an area of 0.02 mm^2 within the cell and the fluorescence sedimentation profile was produced by moving the beam along the length of the cell. Fluorescence light was monitored with photomultiplier optics installed 5 cm above the cell. Primary laser light was suppressed by a light trap and filters. Scans of the cells were controlled and recorded by an Apple II microcomputer.

DNA-dependent RNA polymerase II activity measurements on differing nucleic acid templates

Polymerase II activity measurements on different nucleic acid templates were carried out in a buffer solution containing 10 mM Tris-HCl, pH 7.9, 5 mM $MgCl_2$, 50 mM $(NH_4)_2SO_4$, 0.5 mg/ml BSA, 0.4 mM ATP, CTP, GTP, and 3 µCi of (5-^{3}H) UTP having a specific activity of 20.5 Ci/mmol (New England Nuclear Chemicals, Dreieich, FRG). Assays were performed in triplicate at 37°C for 10 min with 0.6 µg of the indicated substrate in a total volume of 25 µl. The enzyme concentration was 200 nM. To measure incorporation of radioactive label aliquots from the assay mixture were spotted onto 2.5 cm glass microfibre filters (Whatman, GF/C type) which had previously been treated with 0.1 M EDTA. After drying, the filters were collected in an erlenmeyer flask and washed 30 min with 500 ml of 5% TCA and 2% pyrophosphate. After two solution charges, the filters were washed with 500 ml of ethanol, separated into glass scintillation counting vials, dried at 150°C for 1 hr, and then counted with 10 ml of toluene based scintillation cocktail in a Packard Tri-Carb C2425 scintillation counter. In a second assay procedure, unincorporated triphosphates were separated away from incorporated material by means of ascending paper chromatography as described (12). In this system, labeled UTP was observed to have an R_f of 0.86. Radioactivity remaining at the origin was cut out, dried, and counted as above. Results obtained by both methods were consistent. However, the background counts were higher by the washing method. The first method could handle more samples; the second resulted in lower background counts.

Electron microscopy

Buffered reaction mixtures contained 140 µg/ml polymerase II and 20 µg/ml nucleic acids (viroid, virusoid and the 187-bp DNA fragment). Incubation was for 10 min at 37°C, followed by glutaraldehyde fixation (37°C, 10 min, 0.1%

final concentration). Benzyldimethylalkylalkoniumchloride (BAC, Bayer Leverkusen, C_{12}/C_{16} = 60/40) was used as film forming surfactant as described (33). Equal volumes of reaction mixture and BAC (10 µg/ml) were mixed and immediately spread onto water at room temperature. Monolayers were picked up on copper grids covered with a low noise carbon support film. They were positively stained with ethanolic uranyl acetate (0.1 mM in 50% ethanol), dried on filter paper and studied in a Siemens Elmiscope 102 operated in hollow cone dark field.

Fluorescence measurements and spectrophotometric determinations

Fluorescence measurements and titration experiments were performed in an SLM 8000 spectrofluorometer. Reference and sample cells were thermostated at 10°C. Ultraviolet absorption measurements were done in a Beckman UV 5260.

RESULTS

Viroid-polymerase complexes under conditions of excess viroid

Fig. 1A shows the results of a typical analytical ultracentrifugation experiment to determine an equilibrium binding constant between purified viroid RNA and DNA-dependent RNA polymerase II. Viroid-polymerase complexes are separated from the excess free viroid by the difference in their respective sedimentation rates. By estimating (the dashed lines in the figure) the relative heights of the sedimenting bands and knowing the initial concentrations and the relative absorption coefficients of viroid and polymerase, an association constant (K_a) can be calculated (31). The advantage of this type of experiment as opposed to filter binding experiments is that, with an excess of the slow migrating component in the mixture, equilibrium is maintained throughout the experiment. Possible artifacts owing to filtration rate and washing in various filter binding methods are avoided. Multiple scans in the same experiment can be evaluated and averaged.

When the enzyme concentration (and hence the complex concentration) is small as compared to the total viroid concentration, it is difficult to estimate the baseline position of the faster moving upper band. Fig. 1B shows a modification of the ultracentrifugation method which is useful in such cases. By filling the two sides of a double sector centrifugation cell to slightly different heights, a pseudo-differential scan of the moving boundaries can be obtained. The clearer separation of bands into peaks (whose areas can be shown to be proportional to the concentration of the sedimentating components) makes possible a straight forward evaluation of K_a as in Fig. 1A.

Fig. 2 summarizes the results obtained in binding experiments where the

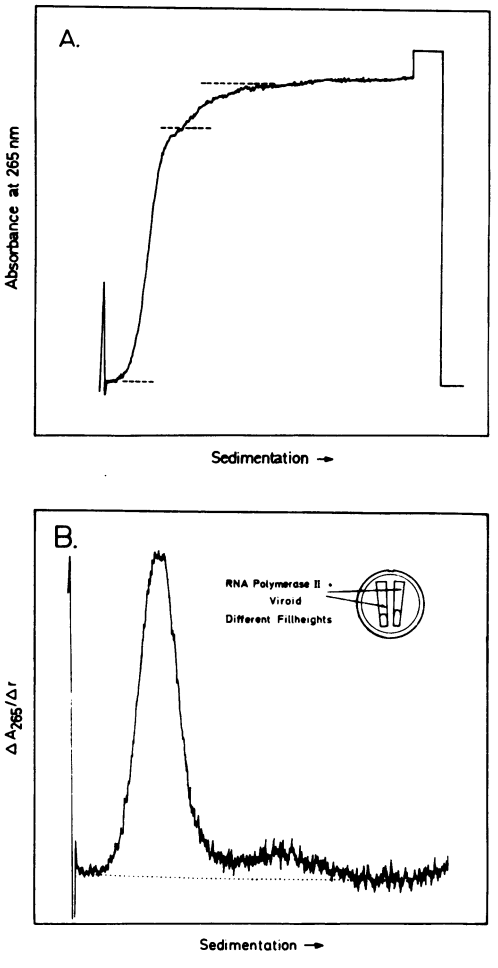

Fig. 1: Analytical ultracentrifugation determination of the equilibrium association constant for the viroid-polymerase interaction.
Panel A shows a scan of an analytical ultracentrifuge cell containing viroid and RNA polymerase II at concentrations of 2.27×10^{-7} and 4.3×10^{-8} M. The faster moving upper band contains both the viroid-polymerase complex as well as unbound enzyme.
Panel B shows a pseudo-differential profile of the unevenly filled cell (diagrammed to the right).

viroid concentration was kept at least 3 times the enzyme concentration. When a 1:1 viroid-to-polymerase stoichiometry is assumed, this figure shows that the observed equilibrium constant, K_a, is dependent on the total enzyme concentration. The dashed line in the figure represents the best-fit linear regression line for these data. Extrapolation to an infinitely dilute enzyme concentration yields a K_a for the viroid-polymerase interaction of 1.9×10^{7} M^{-1} The data presented in this figure are limited in that below approx. 3×10^{-8} M enzyme concentration, the size of the complex band becomes too small to follow accurately in the ultraviolet absorbance scanning mode used in these experiments. The observed equilibrium constant decreases as a function of increasing enzyme concentration. This phenomenon is difficult to interpret quantitatively

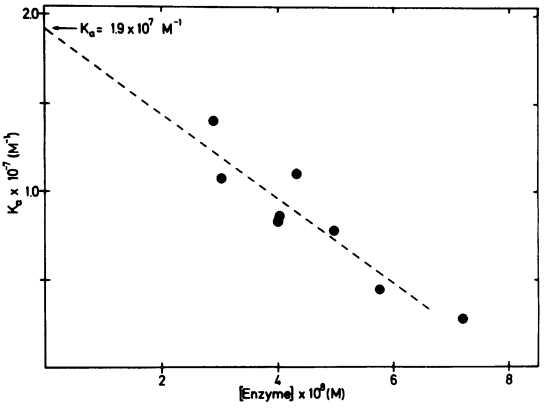

Fig. 2: Observed K_a as a function of enzyme concentration.
The observed equilibrium constant, K_a, is plotted as a function of enzyme concentration. The dashed line represents the best-fit linear regression of the data. The y-intercept of $1.9 \pm 0.5 \times 10^7\ M^{-1}$ corresponds to K_a for the viroid-polymerase interaction at infinitely dilute enzyme conditions. The coefficient of determination is 0.86.

and may come about as the result of the Johnston-Ogsten effect in a two component system. Such dependence was not observed for the other species studied here, probably because of their weaker binding affinities.

Viroid-polymerase complexes under conditions of excess enzyme

With higher enzyme-to-viroid ratios a different phenomenon is observed. The faster moving complex containing band is observed to split into two bands. Fig. 3 shows the results obtained in analytical ultracentrifuge experiments where twofold (panel A) and sixfold (panel B) molar excesses of polymerase over viroid were used. As the excess of polymerase over viroid is increased, the faster moving complex band initially appears to be more rounded at its upper edge. As the ratio is increased further, a separate faster moving band begins to be distinguishable (Fig. 3A). At concentrations of polymerase six times that of the viroid, a large fast moving (26S) band dominates (Fig. 3B) and only a much smaller band (composed at least partially of unbound enzyme) lags behind. The size of the laging band in Fig. 3B cannot be explained only by the presence of free enzyme. One method of determining the composition of these bands was to measure the A_{265}/A_{280} ratio across the moving boundaries during the course of the experiments (31). The results of such determinations and the $S_{20,w}$ values of the bands are summarized in Table 1.

The spectral ratios (A_{265}/A_{280}) observed in the ultracentrifuge for viroid

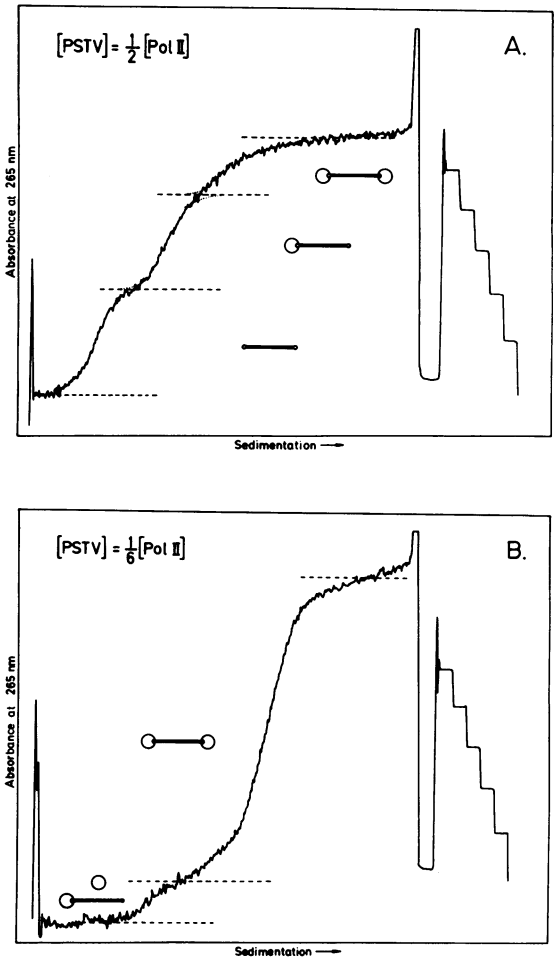

Fig. 3: Sedimentation profiles of viroid and viroid-polymerase complexes under conditions of excess enzyme. The ultraviolet absorbance profiles shown here were obtained when 2.2×10^{-7} M viroid was centrifuged with a twofold (panel A) or sixfold (panel B) excess of polymerase enzyme in the sedimentation buffer. The dashed lines delineate the boundaries observed. The ball and stick drawings (enzyme and viroid, respectively) in the figure diagrammatically summarize the interpretation of these data with respect to the free viroid and viroid-polymerase complexes observed in the experiments. The sedimentation values and spectral characteristics of these bands are described in Table 1.

or polymerase II alone are in good agreement with their values determined in a spectrophotometer. The 15S complex I appears to be composed of viroid and enzyme in a 1:1 molar ratio. The observed value is slightly less than the calculated ratio due to the presence of a small amount of unbound enzyme. The polymerase II migrates slightly faster than complex I (18S as opposed to 15S). Complex II with a sedimentation value of 26S has a lower A_{265}/A_{280} ratio than complex I. The stoichiometry of two enzyme molecules bound to a single viroid is consistent with this observation as well as the data obtained from ultracentrifugation experiments when sample fluorescence was monitored (see below).

Analytical ultracentrifugation with fluorescence detection

In addition to observing viroid and viroid-polymerase complex sedimentation

Table 1: Sedimentation values and spectral characteristics of viroid, DNA-dependent RNA polymerase, and viroid-polymerase complexes[a)]

species[b)]	$S_{20,w}$	A_{265}/A_{280} (observed)	A_{265}/A_{280} (calculated)
Viroid (V)	6.6	1.8	
Polymerase II (E)	18	0.6	
Complex I (VE)	15	1.3	1.52
Complex II (EVE)	26	1.1	1.34

a)Experiments were performed in a buffered 25% glycerol solution (see Methods) and are corrected by the viscosity factor, $\eta/\eta_0 = 2.6$.
b)The abbreviations in parenthesis below the complexes listed here are (VE) for viroid-enzyme and (EVE) for enzyme-viroid-enzyme (see Discussion).

by UV absorbance, the fluorescence properties of these species when complexed with dyes could also be measured in the analytical ultracentrifuge. Under conditions like those shown in Fig. 2 and with an enzyme concentration of 1.7×10^{-8} M, the enzyme-viroid equilibrium association constant was determined to be 2.2×10^{7} M^{-1}. This is in good agreement with the overall data shown in Fig. 2. Fig. 4 shows two different fluorescence sedimentation profiles measured under solution and concentration conditions analogous to those shown in Fig. 3. These experiments measure the fluorescence of intercalated ethidium homodimer. The fluorescence efficiency of the free dye was only approx. 10% that of the bound. The equilibrium constant of the ethidium homodimer-viroid interaction was greater than 10^{8} M^{-1} under the conditions used in these experiments. The sedimentation value of PSTV decreased in the presence of the marker dye. The $S_{20,w}$ values given in the text have been normalized to bring them into consistency with the values observed with the UV detection ultracentrifugation system. Control experiments containing only dye and polymerase II showed that with these conditions, free polymerase was not observed and therefore does not contribute to the band heights in the profiles. As previously in Fig. 3A, with a twofold excess of enzyme, three sedimenting bands are observed. The 20S band appears as the result of mixing between complex I and II. Where a sixfold excess of the polymerase enzyme is used (cf. Fig. 3B) a single larger sedimenting band is seen with only a small amount of trailing. The difference between the slow band observed in Fig. 3B and the indistinct trailing here from the major band at 26S illustrates that a major

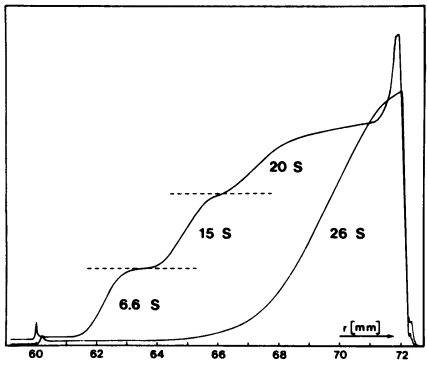

Fig. 4: Sedimentation profiles of viroid and viroid-polymerase complexes as observed by fluorescence detection. The fluorescence intensity (in arbitrary units) is shown here for two different experiments as a function of radius (r). In both experiments the viroid concentration was 2.2×10^{-7} M and ethidium homodimer was present at a concentration of 1.1×10^{-6} M. The leftmost scan where three bands are separated by dashed lines (6.6, 15, and 20S respectively) contained DNA-dependent RNA polymerase II in twofold molar excess over the viroid concentration (analogous to Fig. 3A). When a sixfold excess of enzyme is added (rightmost scan; analogous to Fig. 3B) only a single broader band (26S) is observed. Experiments were performed in parallel using 3 mm cells.

component from the band in Fig. 3B is the free enzyme in excess over the viroid.

Attempts to monitor complex formation by direct fluorometric measurements

If a fluorescence quenching or fluorescence transfer could be measured as a function of viroid-polymerase complex formation, another method would be available to determine the equilibrium binding constant and reaction stoichiometry. Several experiments were undertaken to measure such phenomena. In the simplest approach a polymerase solution was irradiated at 293 nm (to minimize the intrinsic filter effect of the enzyme itself) and the emission fluorescence of the tryptophan residues was measured at their maximum of 333 nm as a function of increasing amounts of viroid RNA or calf thymus DNA (see below) in the solution. No significant change in fluorescence intensity was observed. In another series of experiments, ethidium bromide intercalated into the viroid was used as a fluorescence marker. If in the polymerase binding process, tryptophan residues were sufficiently close (50 Å) to the intercalated ethidium bromide molecules, a Förster transfer from the donor tryptophan to the acceptor ethidium might be anticipated (34). When tryptophan was excited at 293 nm and ethidium emission was monitored at 600 nm with and without the polymerase enzyme present, however, no detectable fluo-

rescence transfer was observed. One possible reason for this could be that the ethidium bromide molecules were displaced from the viroid in the process of polymerase binding. However, titration of the viroid with ethidium bromide in the presence and absence of the enzyme showed no difference in the amount of ethidium bromide that the viroid was capable of binding.

Comparison of viroid with other nucleic acids in their interaction with DNA-dependent RNA polymerase II

Table 2 summarizes the binding constants and template activities observed for the polymerase enzyme with viroid and other nucleic acid templates. Single stranded RNA (cucumber mosaic virus associated, ssCARNA5) showed approximately the same degree of binding to the enzyme as double stranded DNA (187-bp fragment). Viroid-polymerase binding was by comparison more than two times as strong. Binding strength was not directly related to the ability of the nucleic acid to act as a template. DNA in this case was five to ten times as good a template as the viroid RNA. However, among all of the RNA templates tested, viroid was the most effective template. This is consistent with the previously shown ability of the polymerase to produce full-length viroid copies in vitro (12). In spite of the structural similarities between viroids and virusoids, the velvet tobacco mottle virusoid showed no activity as a template. Moreover, its binding constant of 2.5×10^6 M^{-1} was significantly less than that observed for PSTV. The only other RNA species which gave incorporation levels above background was the ssCARNA5. Neither dsCARNA5 nor the tRNA tested here gave any significant level of template activity or enzyme binding.

Electron microscopy of polymerase-nucleic acid interactions

Fig. 5 shows electronmicrographs of the complexes observed between polymerase II and viroid (panel a), virusoid (panel b), and the 187-bp DNA fragment (panel c). In each case, most of the polymerase binding occurs at the ends of the rod-like nucleic acids. With the twofold molar excess of enzyme used here, both 1:1 and 2:1 enzyme to nucleic acid stoichiometries are seen (cf. Fig. 3A).

DISCUSSION

The in vitro model system used here to investigate viroid replication is premised on two observations. First, it is known that the fungal toxin, α-amanitin, inhibits viroid replication at in vivo concentrations of 10^{-8} M (11). The low toxin concentration at which such inhibition occurs strongly suggests that DNA-dependent RNA polymerase II must be involved in viroid replication. Second, partially purified polymerase II from wheat germ has been shown to be

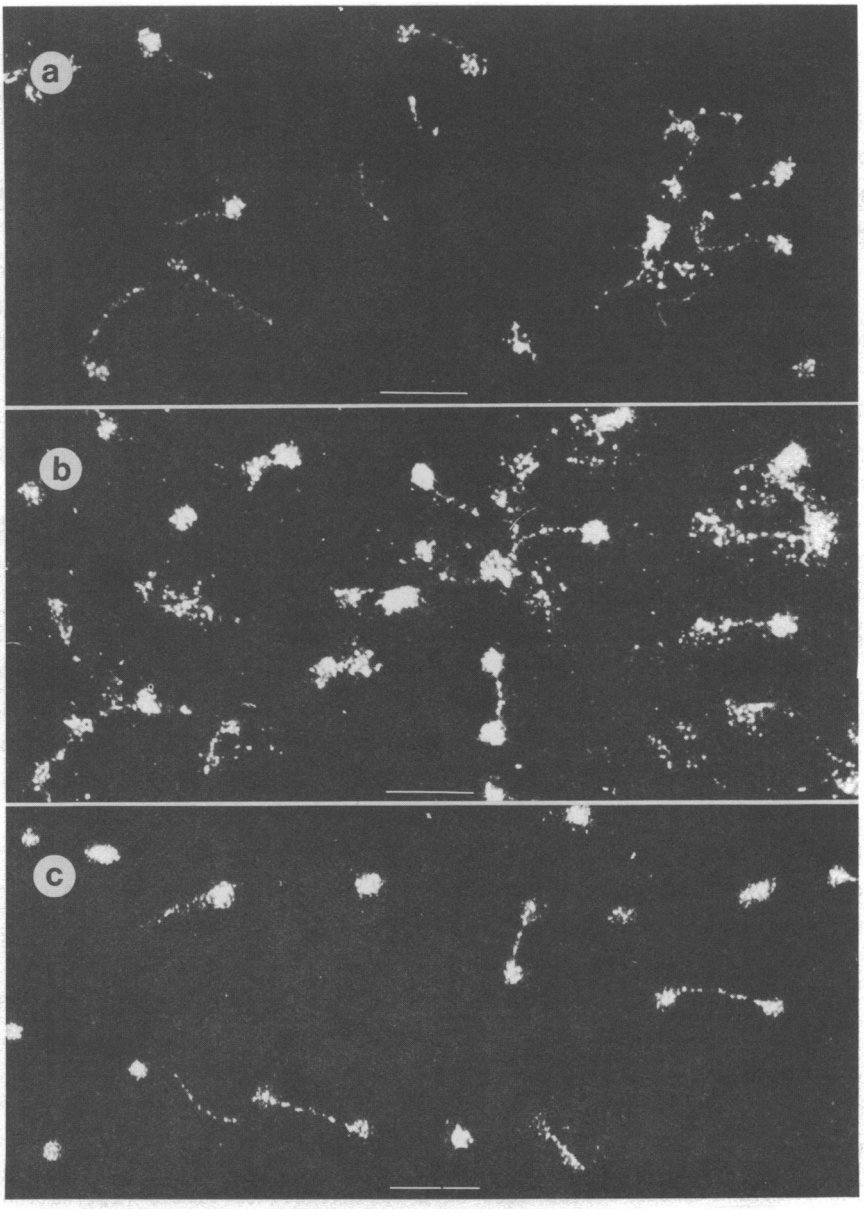

Fig. 5: Electronmicrographs of polymerase-nucleic acid interactions. Electronmicrographs of the complexes observed between DNA-dependent RNA polymerase II and PSTV (panel a), VTMoV virusoid (panel b), and the 187-bp fragment (panel c) are shown here. The polymerase enzyme was in two-fold molar excess over the nucleic acids. The bar in each of the figures represents 50 nm.

Table 2: Interaction of DNA-dependent RNA polymerase II from wheat germ with different nucleic acids

nucleic acid	relative template activity[a)]	binding constant[b)] (K_a x 10^{-6} M^{-1})
potato spindle tuber viroid (PSTV)	9	19.0
velvet tobacco mottle virusoid (VTMoV RNA2)	0	2.5
double-stranded cucumber mosaic virus associated RNA5 (dsCARNA5)	0	0.2
single-stranded cucumber mosaic virus associated RNA5 (ssCARNA5)	1	7.6
tRNA (*E. coli*)	0	0.3
187 base pair DNA	46	7.1
calf thymus DNA	100	n.a.[c)]

a)Normalized to the activity observed with calf thymus DNA (approx. 1.5x 10^5 cpm by the filter washing assay, see Methods).
b)Determined by analytical ultracentrifugation and UV monitoring as in Fig. 1.
c)Not available owing to the size heterogenity of the nucleic acid.

able to produce specific full-length viroid copies *in vitro* (12). Our findings here support and extend this observation by showing substantially larger incorporation rates than previously observed (12) even in the absence of Mn^{+2}. Given these findings, it was expected that wheat germ DNA-dependent RNA polymerase II would show a high binding affinity for viroid RNA. When compared, however, with equilibrium binding constants measured for polymerase-promotor interactions (typically, 10^9 to 10^{12} M^{-1} reviewed in 35), the observed K_a for the viroid-polymerase interaction is rather small. There are several possible explanations for this finding. It may be that an additional binding or recognition protein from the host cell is necessary to obtain tight viroid-polymerase binding. Alternatively, the low binding constant could be an accurate

reflection of the slow replication of viroids *in vivo* during the course of viroid caused diseases. Viroid copy number in severely infected cells is known to be as high as 10,000 (36). The low binding constant may indeed explain the ability of the viroid to accumulate to such high copy numbers, without completely blocking the normal transcription of the cell.

One approach to evaluating the binding data presented in Table 2 is to try to determine what fraction of the observed binding might be caused by non-specific interactions. The viroid RNA is foreign to the cell. Moreover, because it is RNA, it is likely for this reason alone to be less tightly bound by an enzyme that normally recognizes DNA. The binding constant observed between polymerase and *E. coli* tRNA is 3×10^5 M^{-1}. If this is taken as a non-specific level of interaction, the viroid-polymerase interaction (1.9×10^7 M^{-1}) appears by comparison much stronger. A similar comparison can be made to DNA. The 187-bp DNA fragment contains the bacterial tetracycline resistance gene repressor binding site (37). Its non-specific binding to the eukaryotic polymerase II is only half so strong as that of the viroid RNA.

It should also be noted that the virusoid (VTMoV RNA2) has structural similarities to PSTV (3,38). If RNA secondary structure played a major role in polymerase binding, it would be expected that the binding constant of these two species would be similar. This is not the case. Moreover, virusoid is also inactive as a template for the enzyme. This, taken with the observation that viroid template activity was not destroyed by heat denaturation and quick cooling (results not shown) suggests that a particular sequence on the viroid is being recognized and bound by the polymerase enzyme. The overall viroid secondary structure consisting of helical regions and interspersed loops does not appear to play a decisive role in polymerase binding or the early steps of replication.

The fluorescence detection analytical ultracentrifuge system is at least two orders of magnitude more sensitive than the ultraviolet. Because of this, it was envisioned that the K_a at very low enzyme concentrations (below 3×10^{-8} M) could be investigated with this instrument. The results obtained by this method suggest that the K_a for the formation of the viroid-polymerase complex is 2.2×10^7 M^{-1}. This result supports the data presented in Fig. 2. It is not explicitly included there, however, because it may be that the intercalated dye disturbs the binding equilibrium dependent upon its concentration and the concentrations of other components in the system. The fluorescence measurements presented here (see Fig. 4) are limited by the necessity of including a non-covalently bound dye in excess. The qualitative observations made with this technique, however, do show that the two different binding com-

plexes observed at high enzyme concentration are not caused by enzyme aggregation.

The electronmicrographs (Fig. 5) provide visual evidence of both specific and non-specific protein-nucleic acid interactions (39). Equilibrium thermodynamic calculations, however, cannot be made from such pictures, and hence relative binding strengths cannot be determined. The "ball and stick" diagrammatic representation of the 1:1 and 2:1 enzyme-to-viroid binding stoichiometries (see Fig. 3A,B) were suggested by the electronmicrographs shown in Fig. 5. Since the 2:1, 26S complex II is observed only at high enzyme-to-viroid ratios and high enzyme concentration, the equilibrium constant for its formation must be much smaller than the K_a determined here for the 1:1 viroid-polymerase complex I. This suggests that complex II is not physiologically significant. This also indicates that binding at one of the ends must be non-specific. Such an interpretation is also supported by the fact that binding at the ends of the nucleic acid is observed for the virusoid and 187-bp DNA. Only non-specific levels of binding are observed for these species in the ultracentrifuge.

FOOTNOTES

*Present address: CIBA-GEIGY Corp., P.O. Box 12257, Research Triangle Park, NC 27709-2257, USA.

**The work presented here is in partial fulfillment of the requirements for the Ph.D. degree.

#To whom reprint requests should be addressed.

[1]The abbreviations used in the text are: PSTV, potato spindle tuber viroid; VTMoV, velvet tobacco mottle virusoid; ssCARNA5, single stranded cucumber mosaic virus associated RNA5; dsCARNA5, double stranded cucumber mosaic virus associated RNA5.

ACKNOWLEDGEMENTS

We acknowledge the skillful technical assistance of Ms. B. Göbel and U. Schäfer and the help of Ms. H. Gruber in preparing the manuscript. This work was supported by grants from the Deutsche Forschungsgemeinschaft and Fonds der Chemischen Industrie. One of us (T.C.G.) is a post doctoral fellow of the Alexander von Humboldt-Stiftung.

REFERENCES

1. Sänger, H.L. (1982) in: Encyclopedia of Plant Physiology New Series, Parthier, B and Boulter D., Eds., Vol. 14B, pp. 368-454 Springer-Verlag, Berlin.
2. Diener, T.O. (1984) Trends Biochem. Sci. 9, 133-136.
3. Riesner, D., Colpan, M., Goodman, T.C., Nagel, L., Schumacher, J., Steger, G., and Hofmann, H. (1983) Journal of Biomolecular Structure and Dynamics 1, 669-688.

4. Diener, T.O. (1979) "Viroids and Viroid Diseases" John Wiley and Sons, New York.
5. Ohno, T., Takamatsu, N., Meshi, T., and Okada, Y. (1983) Nucleic Acids Res. 11, 6185-6197.
6. Kiefer, M.C., Owens, R.A., and Diener, T.O. (1983) Proc. Natl. Acad. Sci., U.S.A. 80, 6234-6238.
7. Gross, H.J., Domdey, H., Lossow, C., Jank, P., Raba, M., Alberty, H., and Sänger, H.L. (1978) Nature 273, 203-208.
8. Riesner, D., Henco, K., Rokohl, U., Klotz, G., Kleinschmidt, A.K., Domdey. H., Jank, P., Gross, H.J., and Sänger, H.L. (1979) J. Mol. Biol. 133, 85-115.
9. Gross, H.J. and Riesner, D. (1980) Angew. Chem. Int. Ed. Engl. 19, 231-243
10. Riesner, D., Steger, G., Schumacher, J., Gross, H.J., Randles, J.W., and Sänger, H.L. (1983) Biophys. Struct. Mech. 9, 145-170.
11. Mühlbach, H.P., and Sänger, H.L. (1979) Nature 278, 185-188.
12. Rackwitz, H-R., Rohde, W., and Sänger, H.L. (1981) Nature 291, 297-301.
13. Zaitlin, M., Niblett, C.L., Dickson, E., and Goldberg, R.B. (1980) Virology 104, 1-9.
14. Branch, A.D. and Dickson, E. (1980) Virology 104, 10-26.
15. Branch, A.D., Robertson, H.D., and Dickson, E. (1981) Proc. Natl. Acad. Sci., U.S.A. 78, 6381-6385.
16. Rhode, W. and Sänger, H.L. (1981) Biosci. Rep. 1, 327-336.
17. Owens, R.A., and Diener, T.O. (1982) Proc. Natl. Acad. Sci., U.S.A. 79, 113-117.
18. Branch, A.D., and Robertson, H.D. (1984) Science 223, 450-455.
19. Colpan, M., Schumacher, J., Brüggemann, W., Sänger, H.L., and Riesner, D. (1983) Anal. Biochem. 131, 257-265.
20. Colpan, M. and Riesner, D. (1984) J. Chromatogr., in press.
21. Schumacher, J., Randles, J.W., and Riesner, D. (1983) Anal. Biochem. 135, 288-295.
22. Randles, J.W., Davies, C., Hatta, T., Gould, A.R., and Francki, R.I.B. (1981) Virology 108, 111-123.
23. Haseloff, J. and Symons, R. (1982) Nucleic Acids Res. 10, 3681-3691.
24. Diaz-Ruiz, J.R. and Kaper, J.M. (1977) Virology 80, 204-213.
25. Richards, K.E., Jonard, G., Jacquemond, M., and Lot, H. (1978) Virology 89, 395-408.
26. Hillen, W., Klein, R.D., and Wells, R.D. (1981) Biochemistry 20, 3748-3756.
27. Jendrisak, J.J. and Burgess, R.R. (1975) Biochemistry 14, 4639-4645.
28. Jendrisak, J.J. and Burgess, R.R. (1977) Biochemistry 16, 1959-1964.
29. Dynan, W.S. and Burgess, R.R. (1979) Biochemistry 18, 4581-4588.
30. Flossdorf, J. (1980) Makromol. Chem. 181, 715-724.
31. Krauss, G., Pingoud, A., Boehme, D., Riesner, D., Peters, F., and Maass G. (1975) Eur. J. Biochem. 55, 517-529.
32. Rappold, W. and Riesner, D., manuscript in preparation.
33. Vollenweider, H.J., Sogo, J.M., and Koller, T. (1975) Proc. Natl. Acad. Sci. U.S.A. 72, 83-87.
34. Cantor, C.R. and Schimmel, P.R. (1980) "Biophysical Chemistry", Vol.2, 448-454, W.H. Freeman and Co., San Fracisco.
35. Wu, C.W. and Tweedy, N. (1982) Molecular and Cellular Biochem. 47, 129-149
36. Schumacher, J., Sänger, H.L., and Riesner, D. (1983) EMBO J. 2, 1549-1555.
37. Hillen, W., Klock, G., Kaffenberger, I., Wray, L.V., and Reznikoff, W.S. (1982) J. Biol. Chem. 257, 6605-6613.
38. Riesner, D., Kaper, J.M., and Randles, J.W. (1982) Nucleic Acids Res. 10, 5587-5598.
39. Klotz, G., Rackwitz, H-R., and Sänger, H.L. (1982) 10th Int. Congress Electron Microscopy, pp. 75-76.